

Title	Urban PM2.5 exacerbates allergic inflammation in the murine lung via a TLR2/TLR4/MyD88-signaling pathway
Author(s)	He, Miao; Ichinose, Takamichi; Yoshida, Yasuhiro; Arashidani, Keiichi; Yoshida, Seiichi; Takano, Hirohisa; Sun, Guifan; Shibamoto, Takayuki
Citation	Scientific Reports (2017), 7
Issue Date	2017-09-08
URL	http://hdl.handle.net/2433/228158
Right	© The Author(s) 2017.; This article is licensed under a Creative Commons Attribution 4.0 International License, which permits use, sharing, adaptation, distribution and reproduction in any medium or format, as long as you give appropriate credit to the original author(s) and the source, provide a link to the Creative Commons license, and indicate if changes were made. The images or other third party material in this article are included in the article's Creative Commons license, unless indicated otherwise in a credit line to the material. If material is not included in the article's Creative Commons license and your intended use is not permitted by statutory regulation or exceeds the permitted use, you will need to obtain permission directly from the copyright holder.
Type	Journal Article
Textversion	publisher

SCIENTIFIC REPORTS

OPEN

Urban PM2.5 exacerbates allergic inflammation in the murine lung *via* a TLR2/TLR4/MyD88-signaling pathway

Miao He¹, Takamichi Ichinose², Yasuhiro Yoshida³, Keiichi Arashidani³, Seiichi Yoshida^{1,2}, Hirohisa Takano⁴, Guifan Sun¹ & Takayuki Shibamoto⁵

Nevertheless its mechanism has not been well explained yet, PM2.5 is recognized to exacerbate asthma. In the present study, the roles of toll-like receptor (TLR) 2, TLR4 and MyD88, in exacerbation of allergen-induced lung eosinophilia caused by urban PM2.5 was investigated. TLR2^{-/-}, TLR4^{-/-}, MyD88^{-/-} deficient and WT BALB/c mice were intratracheally challenged with PM2.5 +/- ovalbumin (OVA) four times at 2-week intervals. PM2.5 increased neutrophil numbers and KC in bronchoalveolar lavage fluid and caused slight peribronchiolar inflammation in WT mice. However, these changes were attenuated, but not completely suppressed in gene-deficient mice, especially in MyD88^{-/-} mice. In WT mice, PM2.5 + OVA exacerbated OVA-related lung eosinophilia. This exacerbation includes increase of IL-5, IL-13, eotaxin and MCP-3; infiltration of eosinophils into the airway submucosa; proliferation of goblet cells in the airway epithelium; and the production of antigen-specific IgE and IgG1 in serum. All these effects were stronger in TLR2^{-/-} mice than in TLR4^{-/-} mice. In MyD88^{-/-} mice, this pro-inflammatory mediator-inducing ability was considerably weak and lung pathology was negligible. These results suggest that urban PM2.5 may exacerbate allergic inflammation in the murine lung *via* a TLR2/TLR4/MyD88-signaling pathway. PM2.5-bound trace microbial elements, such as lipopolysaccharide may be a strong candidate for exacerbation of murine lung eosinophilia.

High concentrations of atmospheric particulate matter less than 2.5 µm in diameter (PM2.5) are common in Asian countries, especially in some Chinese megacities, and various respiratory health problems have become coincident with this^{1,2}. High levels of PM2.5 have been associated with an increase in numbers of chronic obstructive pulmonary disease (COPD) and asthma patients in China and Taiwan³.

Asthma, especially in children, is a chronic disease with airway obstruction, and is characterized by chronic allergic inflammation of the airways with superimposed episodes of acute inflammation⁴. Acute exacerbations are the most clinically significant feature of asthma. They are represented by increase of distal eosinophilic airway inflammation associated with exaggeration of symptoms, such as cough, chest tightness and dyspnoea⁵. PM2.5 is known to be related to the development and exacerbation of asthma. For example, PM2.5 promotes sensitization to common aeroallergens and the development of allergic respiratory diseases⁶. Ambient PM2.5 levels show a positive correlation with upsurges in emergency department visits for asthma^{7,8}, hospital admissions for asthma in children^{9,10}, and worsening wheezing and dyspnoea¹¹. Furthermore, asthma morbidity has been positively associated with daily ambient PM2.5 concentrations, in both warm and cool seasons¹². The composition of PM2.5 may contribute to a higher prevalence and incidence of asthma^{13,14}.

¹Department of Environmental Health, School of Public Health, China Medical University, Shenyang, 110122, China. ²Department of Health Sciences, Oita University of Nursing and Health Sciences, Oita, 870-1201, Japan. ³Department of Immunology and Parasitology, School of Medicine, University of Occupational and Environmental Health, Fukuoka, 807-8555, Japan. ⁴Environmental Health Division, Department of Environmental Engineering, Graduate School of Engineering, Kyoto University, Kyoto, 615-8530, Japan. ⁵Department of Environmental Toxicology, University of California, Davis, California, 95616, USA. Correspondence and requests for materials should be addressed to M.H. (email: mhe@cmu.edu.cn) or T.I. (email: ichinose@oita-nhs.ac.jp)

Elements (µg/mg) Compositions		Trace (ng/ mg) elements		Trace (ng/ mg) elements		Water soluble (µg/mg) components		Microbial (pg/mg) elements	
Si	13	Sc	<9.1	Mo	110	SO ₄ ²⁻	160	LPS	83
Na	4.7	V	60	Sb	90	NO ₃ ⁻	130	β-glucan	410
Al	3.7	Cr	160	Cs	11	CL ⁻	40		
K	18	Mn	510	Ba	71	Na ⁺	4.6		
Ca	4	Ti	370	La	3.5	NH ₄ ⁺	110		
Fe	6.8	Co	8.5	Ce	5.7	K ⁺	17		
Zn	5.4	Ni	72	Sm	<1.7	Mg ²⁺	1.6		
Pb	1.7	Cu	340	Hf	0.3	Ca ²⁺	2.9		
		As	380	W	12				
OC	84	Se	70	Th	<2.5				
EC	182	Rb	68	Cd	28				

Table 1. Concentration of chemical elements, water soluble components, LPS and β-glucan in PM2.5. OC: organic carbon; EC: element carbon.

Anthropogenic PM2.5 contains large amounts of toxic chemicals formed by the combustion of fossil fuel. Chemicals identified to date include polycyclic aromatic hydrocarbons (PAHs), sulfates (SO₄²⁻)/nitrates (NO₃⁻), transition metals (i.e. Fe, Cu, Ni), and microbial elements such as lipopolysaccharide (LPS) and β-glucan^{15,16}.

In our previous work using a murine asthma model, we have shown that urban dust collected from the air in Beijing, China exacerbated ovalbumin (OVA)-associated murine lung eosinophilia¹⁷, as did PM2.5 collected from the air in Shenyang, China^{15,16} and PM2.5-rich dust collected from the air in Fukuoka, Japan¹⁸. However, the precise exacerbating factors contained within urban PM2.5 and the mechanisms of action are not fully understood. Therefore, studies to clarify the mechanisms involved in exacerbation of murine lung eosinophilia are necessary.

Toll-like receptors (TLRs) expressed by antigen presenting cells (macrophages, dendritic cells) and other various cells (e.g., airway epithelial cells) are innate immune sensors, which recognize microbial pathogen-associated molecular patterns (bacteria, fungi, and virus structures) as well as endogenous danger molecules from host cells. TLR2 is a receptor for β-glucans of fungi and peptidoglycans of Gram-positive bacteria¹⁹, while TLR4 detects LPS²⁰. Myeloid differentiation factor 88 (MyD88) is a downstream signalling adapter protein and essential for cytokine production in response to TLR ligands²¹. We have recently reported that MyD88 downstream of TLR2 and TLR4 is a key protein in OVA-induced exacerbation of murine lung eosinophilia by Asian sand dust²².

Investigation of the role of TLR2, TLR4 and MyD88 in the exacerbation of allergen-induced lung eosinophilia caused by PM2.5 was conducted to clarify the relationship between microbial elements present in PM2.5 and disease exacerbation in a mouse model of asthma. Gene deficient (TLR2^{-/-}, TLR4^{-/-} and MyD88^{-/-}) and wild type (WT) BALB/c mice were intratracheally challenged with OVA and/or PM2.5 in the present study.

Results

Components in PM2.5 samples. PM2.5 includes constituents such as metal, sulfate, organic carbon (OC), and elemental carbon (EC); its chemical composition varies geographically depending on natural and/or anthropogenic generating sources. Table 1 shows the results of the major elements analysis. A total of 8 major elements were identified, along with OC and EC. In PM2.5, the concentration of K (18 μg/mg) was the highest, followed by Si (13 μg/mg), Fe (6.8 μg/mg), Zn (5.4 μg/mg), Na (4.7 μg/mg), Ca (4 μg/mg), Al (3.7 μg/mg), and Pb (1.7 μg/mg). OC and EC were 84 μg/mg and 182 μg/mg in PM2.5, respectively.

Table 1 also shows the results of the minor elements analysis. Mn had the highest concentration (510 ng/mg), followed by As (380 ng/mg), Ti (370 ng/mg), Cu (340 ng/mg), Cr (160 ng/mg), Sb (90 ng/mg), Ni (72 ng/mg), Ba (71 ng/mg), Se (70 ng/mg), Rb (68 ng/mg), V (60 ng/mg), Cd (28 ng/mg), W (12 ng/mg), Cs (11 ng/mg), Co (8.5 ng/mg), Ce (5.7 ng/mg) and La (3.5 ng/mg).

The anion concentrations were SO₄²⁻ (160 μg/mg), NO₃⁻ (130 μg/mg), and Cl⁻ (40 μg/mg). The cation concentrations were NH₄⁺ (110 μg/mg), K⁺ (17 μg/mg), Na⁺ (4.6 μg/mg), Mg²⁺ (1.6 μg/mg), and Ca²⁺ (2.9 μg/mg). The microbial levels of LPS and β-glucan were 83 pg/mg and 410 pg/mg, respectively.

Table 2 shows the results of the PAHs analysis. A total of 14 PAHs was identified. The concentration of BbF (448 μg/g) was the highest, followed by BeP (233 μg/g), DBA (217 μg/g), PYR (208 μg/g), FLU (153 μg/g) and BaA (108 μg/g). The concentration of the most potent carcinogen, BaP, was 61.1 μg/g.

Inflammatory cells in BALF. As shown in Fig. 1, PM2.5 significantly increased macrophages and neutrophils over the control in WT mice, but not significantly increased these cells in TLR2^{-/-}, TLR4^{-/-} and MyD88^{-/-} mice. PM2.5 tended to increase lymphocytes in TLR2^{-/-}, TLR4^{-/-} and MyD88^{-/-} mice. OVA + PM2.5 significantly increased neutrophils, eosinophils and lymphocytes compared to the controls, PM2.5- and OVA-only counterparts in WT mice, TLR2^{-/-} and TLR4^{-/-} mice, but not increased these inflammatory cells in MyD88^{-/-} mice. The eosinophil number in WT mice was greater than in TLR2^{-/-} mice, whereas it was lower in TLR4^{-/-} mice or undetectable level in MyD88^{-/-} mice.

Cytokine and chemokine levels in BALF. As shown in Fig. 2, PM2.5 alone and OVA + PM2.5 significantly increased IL-1β in WT, TLR2^{-/-} and TLR4^{-/-} mice; KC in WT, TLR2^{-/-} and MyD88^{-/-} mice; and MCP-1

PAHs	($\mu\text{g/g}$)
Chrysene (CHR)	83.6
Fluorene (FLU)	153
Benzo[a]anthracene (BaA)	108
Pyrene (PYR)	208
Benzo[a]pyrene (BaP)	61.1
Benzo[k]fluoranthene (BkF)	26.7
Benzo[b]fluoranthene (BbF)	31.7
Dibenzo[a,h]anthracene (DBA)	217
Benzo[e]pyrene (BeP)	233
Benzo[j]fluoranthene (BjF)	448
Perylene	20.1
Benzo[g,h,i]perylene (BPE)	53.3
Indeno[1,2,3-cd]pyrene (IPR)	57.2
Coronene	24.2

Table 2. Concentration of PAHs in PM2.5. PM2.5 and CPM samples were analyzed for PAHs by a HPLC equipped with a fluorescence detector and a 4.0 mm ϕ \times 250 mm column a packed with Wakosil-II 5 C 18HG.

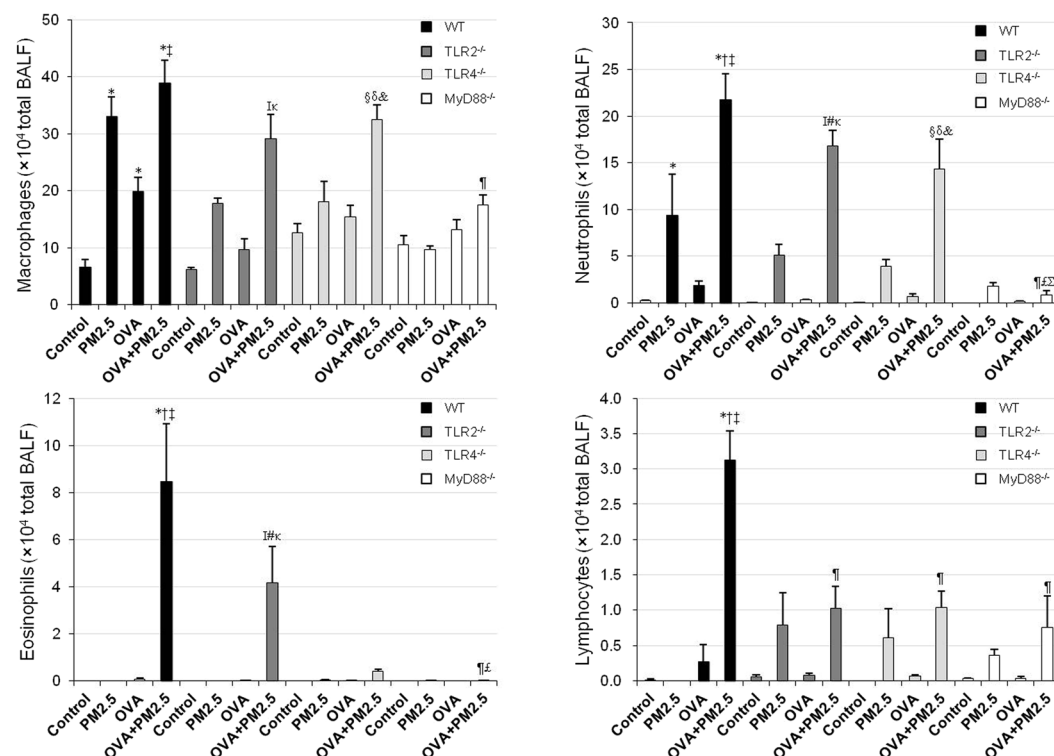


Figure 1. Inflammatory cells in BALF. Differential cell counts were assessed in cytologic preparations stained with Diff-Quik. All values are expressed as mean \pm SE (n = 6). *p < 0.05 vs. WT Control; †p < 0.05 vs. WT PM2.5; ‡p < 0.05 vs. WT OVA; §p < 0.05 vs. WT OVA + PM2.5; ¶p < 0.05 vs. TLR2^{-/-} Control; ¶p < 0.05 vs. TLR2^{-/-} PM2.5; ¶p < 0.05 vs. TLR2^{-/-} OVA; ¶p < 0.05 vs. TLR2^{-/-} OVA + PM2.5; §p < 0.05 vs. TLR4^{-/-} Control; ¶p < 0.05 vs. TLR4^{-/-} PM2.5; ¶p < 0.05 vs. TLR4^{-/-} OVA; ¶p < 0.05 vs. TLR4^{-/-} OVA + PM2.5.

in MyD88^{-/-} mice over the controls. PM2.5 alone tended to increase IL-1 β in MyD88^{-/-} mice and the increased level was same as that of WT mice.

OVA + PM2.5 significantly increased IL-12 in WT, TLR2^{-/-} and TLR4^{-/-} mice and MCP-1 in TLR2^{-/-} and TLR4^{-/-} mice relative to the controls. OVA + PM2.5 also significantly increased Th-2 cytokine IL-5 in WT, TLR2^{-/-} and TLR4^{-/-} mice, IL-13 in WT and TLR2^{-/-} mice, eosinophil-relevant MCP-3 in WT mice compared to the controls, PM2.5- and OVA-only counterpart and eotaxin in WT mice compared to the controls and OVA-only counterpart, but caused less or no secretion of these cytokine and chemokine in MyD88^{-/-} mice. Furthermore, an increase of the above cytokine and chemokine in TLR2^{-/-} mice were higher than those in TLR4^{-/-} mice.

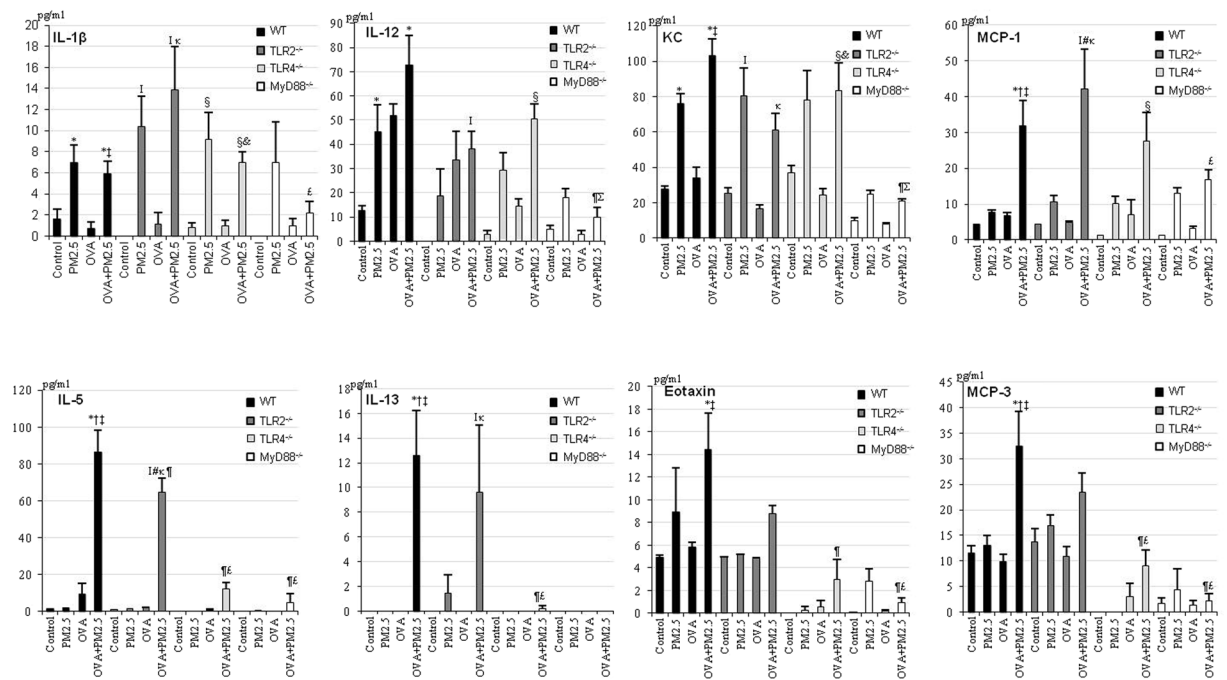


Figure 2. Expression of cytokines and chemokines in BALF. All values are expressed as mean \pm SE (n = 6). *p < 0.05 vs. WT Control; †p < 0.05 vs. WT PM2.5; ‡p < 0.05 vs. WT OVA; §p < 0.05 vs. WT OVA + PM2.5; ¶p < 0.05 vs. TLR2^{-/-} Control; ††p < 0.05 vs. TLR2^{-/-} PM2.5; †††p < 0.05 vs. TLR2^{-/-} OVA; ††††p < 0.05 vs. TLR2^{-/-} OVA + PM2.5; †††††p < 0.05 vs. TLR4^{-/-} Control; †††††p < 0.05 vs. TLR4^{-/-} OVA; †††††p < 0.05 vs. TLR4^{-/-} OVA + PM2.5.

Pathologic changes in the airways. No pathologic alterations were found in the lungs of the control group in WT, TLR2^{-/-}, TLR4^{-/-} and MyD88^{-/-} mice (Fig. 3A,D,G,I). PM2.5 alone caused peribronchiolar inflammation in WT mice (Fig. 3B). Infiltration of inflammatory cells (neutrophils and lymphocytes) into the airway submucosa was observed (arrows). However, the degree of peribronchiolar inflammation was very slight in TLR2^{-/-} and TLR4^{-/-} mice (Fig. 3E,H), but no significant changes in the airway of MyD88^{-/-} mice (Fig. 3K).

OVA + PM2.5 caused proliferation of goblet cells in the airway epithelium in WT mice, TLR2^{-/-} and TLR4^{-/-} mice (Fig. 3C,F,I; thin arrows). However, no significant pathological changes in MyD88^{-/-} mice were observed (Fig. 3L). In the pathological scores, the degree of goblet cell proliferation between groups was WT mice > TLR2^{-/-} mice > TLR4^{-/-} mice > MyD88^{-/-} mice (Fig. 3). OVA + PM2.5 caused infiltration of eosinophils, neutrophils, and lymphocytes into the airway submucosa, especially in WT mice (Fig. 3M). However, no significant pathological changes in the lungs of MyD88^{-/-} mice were observed (Fig. 3P). In the pathological scores, the degrees of eosinophil and lymphocyte infiltration into the airway submucosa between groups were WT mice > TLR2^{-/-} mice > TLR4^{-/-} mice > MyD88^{-/-} mice (Fig. 3). These pathological scores in the OVA + PM2.5 group of WT, TLR2^{-/-}, TLR4^{-/-} and MyD88^{-/-} mice were parallel to the induction levels of Th2 cytokines and eosinophil-relevant chemokines in these groups.

OVA-specific IgE and IgG1 in serum. OVA alone caused no induction of OVA-specific IgE and IgG1. OVA + PM2.5 significantly increased OVA-specific IgE and IgG1 production in WT mice, TLR2^{-/-} and TLR4^{-/-} mice compared to OVA only-hosts, whereas these antibodies were undetectable in MyD88^{-/-} mice in Fig. 4.

Discussion

The results of the present study indicate that the activation of TLR signalling by PM2.5, which leads to inflammatory cytokine production, may result in activation of the innate and adaptive immunity related to Th2 responses. The results of the present study demonstrated that exposure to PM2.5 alone increased neutrophil numbers in BALF and also increased chemokine KC levels in WT mice. The human homologue of KC, IL-8, recruits and activates neutrophils²³. However, these alterations were attenuated although not completely suppressed in TLR2^{-/-}, TLR4^{-/-} and MyD88^{-/-} mice. Pathologically, PM2.5 caused slight peribronchiolar inflammation in WT mice, but more subtle pathological changes were observed in the gene-deficient mice, especially in MyD88^{-/-} animals. These data indicate that PM2.5 is capable of activating the innate immune system in a MyD88-dependent manner. These data also suggest that contaminating trace LPS and TLR2 ligands (β -glucan, etc) in PM2.5 are strong candidates for the active agents in neutrophilic lung inflammation caused by PM2.5. A recent study has reported that PM2.5-induced acute lung inflammation in BALB/c mice might be due, in part, to the production of IL-1 β . The activation of the TLR4/MyD88 signaling pathway and NOD-like receptor family, pyrin domain-containing 3 (NLRP3) might be involved in the production process²⁴. In the present study, PM2.5 increased IL-1 β in WT mice, TLR2^{-/-}, TLR4^{-/-} and MyD88^{-/-} mice. PM2.5 might cause IL-1 β induction through the NLRP3

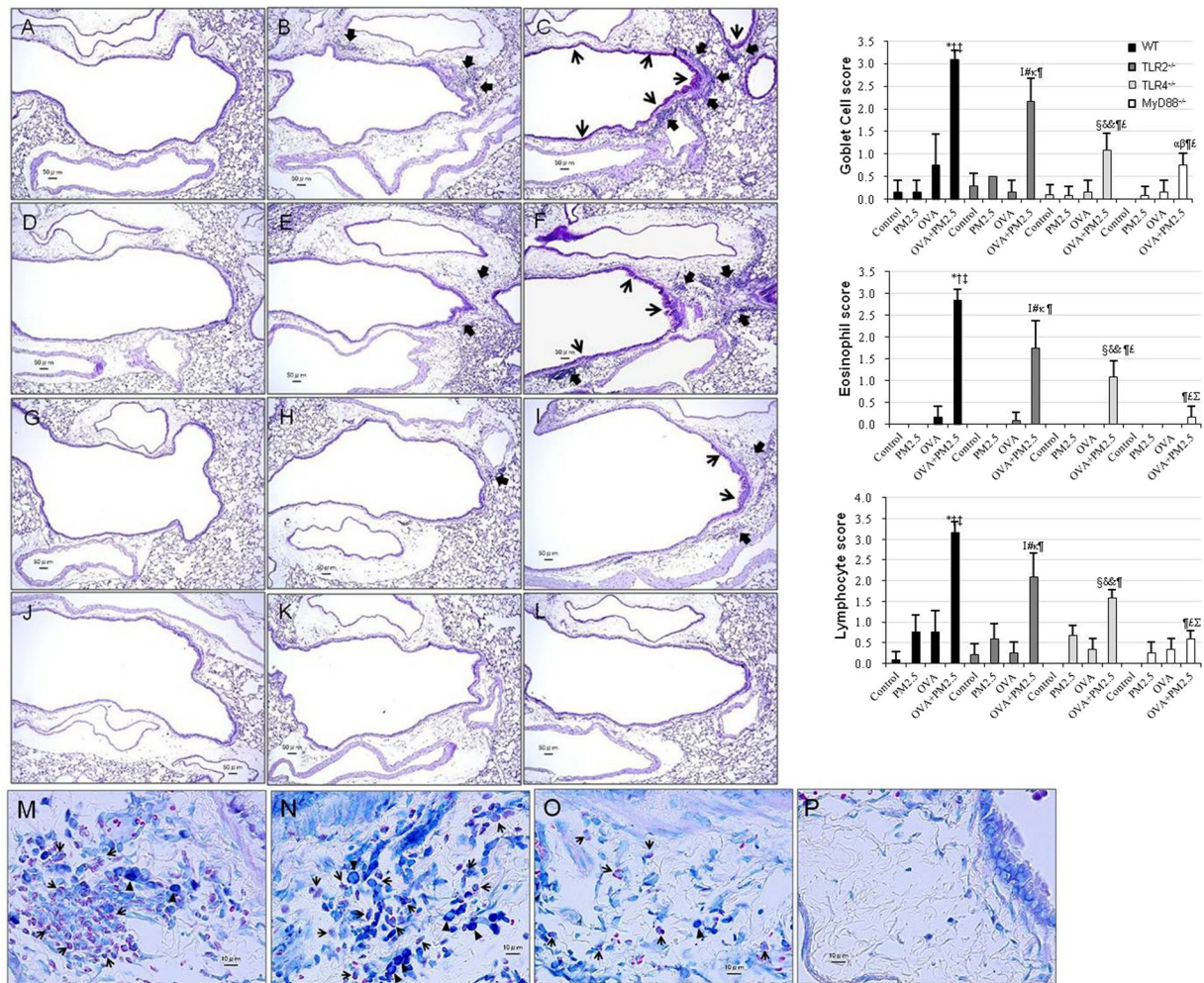


Figure 3. Pathological changes in mice lungs. (A) WT Control; (D) TLR2^{-/-} Control; (G) TLR4^{-/-} Control; (J) MyD88^{-/-} Control: no pathological changes in lungs treated with saline. (B) WT PM2.5: very slight proliferation of airway epithelial cells, and peribronchiolar inflammation due to slight infiltration of inflammatory cells into the submucosa of airways. (C) WT OVA + PM2.5: moderate proliferation of goblet cells (thin arrow) that have mucus stained pink with PAS in the airway epithelium, and moderate to marked infiltration of inflammatory cells (arrow) into the submucosa of airways. Mild to moderate fibrous thickening of the subepithelial layer in the airway also was seen. (E) TLR2^{-/-} PM2.5: proliferation of airway epithelial cells, peribronchiolar inflammation due to very slight infiltration of inflammatory cells (arrow) into the airway submucosa. (F) TLR2^{-/-} OVA + PM2.5: mild to moderate proliferation of goblet cells (arrow) in the airway epithelium, inflammatory cells in the airway submucosa. (H) TLR4^{-/-} PM2.5: no pathological changes in airway epithelial cells and very slight infiltration of inflammatory cells (arrow) into the airway submucosa. (I) TLR4^{-/-} OVA + PM2.5: slight proliferation of goblet cells (thin arrow) in the airway epithelium, and slight infiltration of inflammatory cells (arrow) into the airway submucosa. (K) MyD88^{-/-} PM2.5: no pathological changes in airway epithelial cells and no inflammatory cells in the airway submucosa. (L) MyD88^{-/-} OVA + PM2.5: no significant pathological changes in airway epithelium or airway submucosa. (A–L) PAS stain; Bar = 50 μ m. (M–P) Infiltration of inflammatory cells into the airway submucosa. May-giemsa stain; bar = 10 μ m. (M) WT OVA + PM2.5: marked infiltration of eosinophils into the airway submucosa. (N) TLR2^{-/-} OVA + PM2.5: moderate infiltration of eosinophils. (O) TLR4^{-/-} OVA + PM2.5: slight infiltration of eosinophils. (P) MyD88^{-/-} OVA + PM2.5: no significant pathological changes in the airway submucosa. Arrows show eosinophils with red granules. Triangles show tissue macrophages. Right side graphs: Evaluation of pathological changes in the murine airway. All values are expressed as mean \pm SE (n = 6). *p < 0.05 vs. WT Control; †p < 0.05 vs. WT PM2.5; ‡p < 0.05 vs. WT OVA; §p < 0.05 vs. WT OVA + PM2.5; ¶p < 0.05 vs. TLR2^{-/-} Control; *p < 0.05 vs. TLR2^{-/-} PM2.5; †p < 0.05 vs. TLR2^{-/-} OVA; ‡p < 0.05 vs. TLR2^{-/-} OVA + PM2.5; §p < 0.05 vs. TLR4^{-/-} Control; ¶p < 0.05 vs. TLR4^{-/-} PM2.5; *p < 0.05 vs. TLR4^{-/-} OVA; ‡p < 0.05 vs. TLR4^{-/-} OVA + PM2.5; ¶p < 0.05 vs. MyD88^{-/-} Control; §p < 0.05 vs. MyD88^{-/-} PM2.5.

inflammasome-pathway (MyD88 independent-pathway). It is well known that the inflammasome-pathway is activated by danger signals (peptidoglycan, silica, ATP, uric acid crystal)²⁵.

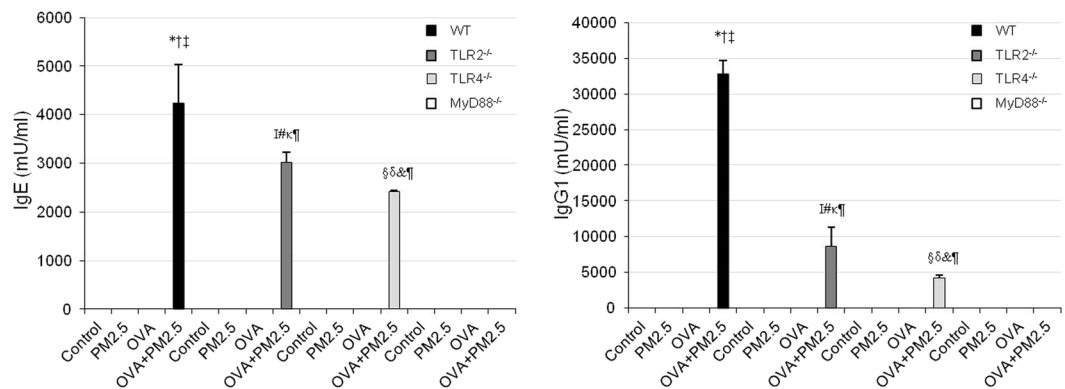


Figure 4. OVA-specific IgE and IgG1 in serum. According to the manufacturer's protocol, 1 U of anti-OVA IgE is defined as 1.3 ng of the antibody, and 1 U of anti-OVA IgG1 as 160 ng of the antibody. Results are expressed as mean \pm SE (n = 6). *p < 0.05 vs. WT Control; †p < 0.05 vs. WT PM2.5; ‡p < 0.05 vs. WT OVA; §p < 0.05 vs. WT OVA + PM2.5; ¶p < 0.05 vs. TLR2^{-/-} Control; ††p < 0.05 vs. TLR2^{-/-} PM2.5; ‡‡p < 0.05 vs. TLR2^{-/-} OVA; §§p < 0.05 vs. TLR4^{-/-} Control; ¶¶p < 0.05 vs. TLR4^{-/-} PM2.5; &p < 0.05 vs. TLR4^{-/-} OVA.

Regarding TLR2 stimuli, hydrogen peroxide (H_2O_2), which is generated during inflammation, induces nuclear translocation of NF- κ B and AP-1, and phosphorylation of p38 MAPK in neonatal rat ventricular myocytes; anti-TLR2 antibody inhibits these effects. H_2O_2 increases NF- κ B activation in TLR2-overexpressing Chinese hamster ovary (CHO) fibroblasts, but not in normal or TLR4-overexpressing CHO cells²⁶. As metal-containing TLR stimuli, TiO_2 nanoparticles activate TLR2 and TLR4, and induce expression of TNF- α and NF- κ B in mouse hippocampal tissues²⁷. Zinc and nickel administration induce inflammatory responses (ICAM-1 and IL-8 induction) in vascular endothelial cells. In these responses, TLR4 plays a dominant role in NF- κ B activation by nickel, but not by zinc²⁸. In the present study, these metals were included in the tested PM2.5 sample (Ti, 370 ng/mg; Ni, 72 ng/mg). From these reports, we speculate that H_2O_2 is generated extracellularly by inflammation, Ti and Ni present in PM2.5 trigger lung inflammation *via* TLRs.

Regarding the relationship between particle size and inflammatory response, overall urban PM2.5-induced inflammatory responses in murine lungs, including those identified in this study, are weaker than those observed in response to coarse PM (PM2.5–PM10 μ m) or fine particles derived from desert dust (2.5 μ m)^{15, 16}. We hypothesize that the differences in these inflammatory responses may be due to the differences in amounts of particle-bound microbial elements, especially LPS. However, we currently have reported that type II alveolar cells might react sensitively to oxidative stress induced by PM2.5 and caused an inflammatory response because the response was suppressed by *N*-acetylcystein (anti-oxidants) but not by Polymyxin B (LPS inhibitor)²⁹. Therefore, the oxidative stress caused by chemical-rich PM2.5 might play an important role in murine lung inflammation in addition to LPS and metals.

In OVA-treated WT mice, PM2.5 exacerbated OVA-related lung eosinophilia along with an increase in Th2 cytokines (IL-5, and IL-13) and chemokines (eotaxin and MCP-3) and infiltration of eosinophils into the airways. Increasing proliferation of goblet cells in the airway epithelium and production of antigen-specific IgE and IgG1 in serum are exacerbated by allergic inflammatory events. These Th2-derived cytokines and chemokines are key mediators in the symptoms of asthma and are critical for the recruitment and survival of eosinophils³⁰, production of antigen-specific antibodies³¹, and the production of mucous cells (e.g., goblet cells) in the bronchial epithelium³². All these effects were stronger in TLR2^{-/-} mice than in TLR4^{-/-} mice. In MyD88^{-/-} mice, this pro-inflammatory mediator-inducing ability was very weak and the lung pathology exhibited negligible effect following exposure to the sample mixtures. These results suggest that TLR2 and TLR4 signalling may be important in the exacerbation of PM2.5-induced lung eosinophilia and that MyD88 is a key adapter molecule in this event. Therefore TLR2- and TLR4-ligands, TLR stimuli (H_2O_2 , metals) and other danger-stimulus might trigger the exacerbation of lung eosinophilia. However, PM2.5-bound LPS may be a strong candidate for exacerbation of lung eosinophilia caused by PM2.5, indicated by the strong inhibition of effects in TLR4^{-/-} mice.

We have recently reported that antigen-induced allergic inflammation in murine lungs was greater in microbial element (LPS, β -glucan)-rich coarse PM than in organic chemical (PAHs)-rich PM2.5 and have suggested that microbial elements have more potent exacerbating effects on the development of lung eosinophilia than do organic chemicals contained in PM2.5¹⁶. We have also reported that heated PM2.5-rich dust—heated at 360 °C to exclude toxic materials, such as microbial and chemical elements—caused less effect on neutrophilic lung inflammation and OVA-induced lung eosinophilia in mice than non-heated PM2.5-rich dust¹⁸. Thus, PM2.5-bound toxic materials are seen to be a key factor for these lung disease enhancements. Therefore, investigation to confirm the phenomenon found by the present study, whether exposure to a mixture of heated PM2.5 and LPS or β -glucan in trace levels causes exacerbation of murine lung eosinophilia or not, is in order.

Conclusion

This study demonstrates that urban PM2.5 may exacerbate allergic inflammation in the murine lung *via* a TLR2/TLR4/MyD88-signaling pathway. PM2.5-bound trace microbial elements, such as LPS may be a strong candidate

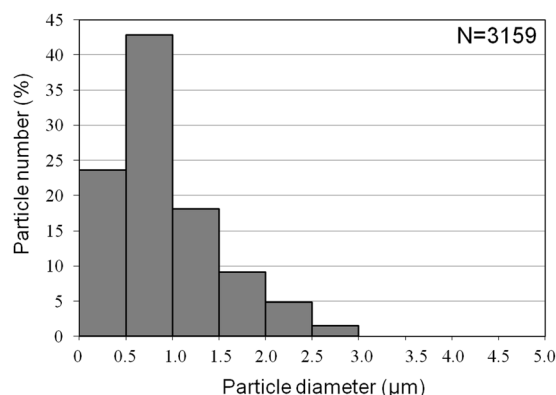


Figure 5. Particle diameter distribution. Particle size was analyzed using a microscope. A total of 3159 particles were measured. Results show the median diameter of PM_{2.5} to be 0.94 μm. The size distribution peaks of PM_{2.5} were at 0.5–1.0 μm.

for exacerbation of murine lung eosinophilia. The results of the present study suggest that inhalation of urban PM_{2.5} is a significant risk factor for inflammatory and allergic lung diseases.

Methods

Sample collection of PM_{2.5}. PM_{2.5} samples collected between Jan 20 and Jan 25, 2015 were obtained from China Medial University, Shenyang, China. In China, a massive haze event (density ranges of PM_{2.5} = 129–291 μg/m³) appeared at this time. The experimental air samples were trapped in a four-stage multi-nozzle cascade impactor (MCI) (Tokyo Dylec Co., Tokyo, Japan). An MCI was used to measure the levels of size-classified mass and elemental concentrations of PM_{2.5} accordance with a previously reported method^{15–18}. The MCI consisted of three stages with 12-orifice and back-up stage. The PM_{2.5} was trapped directly on materials placed behind the jet-nozzles of an MCI set at 20 l/min airflow. The PM_{2.5} collected was transferred to a sterilized dry bottle, which was placed in a germ free desiccator and stored at –30 °C for further use.

Particle size. Figure 5 shows the particle size of the PM_{2.5} analyzed by KEYENCE all-in-one BZ-9000 fluorescence microscope (Osaka, Japan). A total of 3159 particles were counted. The median diameter of the PM_{2.5} particles was 0.94 ± 0.65 μm (M ± SD). The peak of the size distribution was at 0.5–1.0 μm.

Analysis of components in the samples. Thermo Scientific model 61E Trace and ICP-750, Thermo Jarrell-Ash inductively-coupled plasma atomic emission spectroscopy (ICP-AES) (Waltham, MA) was used to analyze the elements. Prior to analysis, samples were treated for acid digestion with mixed acids (68% HNO₃/38% HF/70% HClO₄ = 5/1/1) for 3 h at 180 °C. An ion chromatograph (DX-100, Dionex, Sunnyvale, CA) and ICP-AES (61E Trace, Thermo Jarrell-Ash) were used to analyze the water soluble components.

Analysis of microbial elements in particles. Kinetic assays (Seikagaku Corp., Tokyo, Japan) were applied to measure microbial elements: Endospec ES tested MK for LPS activity and Fungitec G tested MK for β-glucan. Briefly, one ml water suspension of PM_{2.5} (5 mg) was allowed to stand on the bench top at room temperature for 2 h. Subsequently, supernatants recovered were examined for LPS and β-glucan concentrations using Pyro Color-MP Chromogenic Diazo-Coupling Kit (Associates of Cape Cod, Inc., MA, USA).

Analysis of polycyclic aromatic hydrocarbons (PAHs) in particles. A previously reported method^{15–18} was used to analyze PAHs. Briefly, ultrasonic extraction was performed to extract the air samples trapped on the Teflon filter. The samples were extracted twice with a 20 ml portion of dichloromethane at 15 °C. The filtrate obtained from the extract using a No 5 C filter paper was allowed to dryness in the dark, yielding solid residual substances.

The residual substances dissolved in acetonitrile (0.5 ml) were analyzed for PAHs using a Hitachi Model 600 HPLC (Hitachi, Japan). The HPLC was equipped with a Model L-7485 fluorescence detector (Hitachi, Japan) and a 4.0 mmφ × 250 mm column packed with Wakosil-II 5C 18HG (Waka Pure Chemicals Industry, Ltd., Osaka, Japan). An acetonitrile/water (80/20, v/v) solution was used as a mobile phase at 1.5 ml/min. Identification of unknown PAHs was performed by comparing the HPLC retention time and fluorescence/excitation spectra to those of authentic PAHs³³ from Supelco (Bellefonte, PA, USA) and Aldrich Chemical Co., Inc. (Milwaukee, WI, USA)/Tridom Chemical Inc (Hauppauge, NY, USA).

Animals. Homozygous TLR2, TLR4 and MyD88 knockout mice and WT mice (BALB/c parental strain, males) were purchased from Oriental BioService Japan, Inc. (Kyoto, Japan) at 8 weeks of age. Mice were fed with a commercially obtained diet CE-2 (CLEA Japan, Inc., Tokyo) and given water ad libitum. They were placed in plastic cages lined with soft wood chips and kept in a well-controlled room—temperature, 23 °C; humidity, 55–70%, 12 h/12 h light/dark cycle. The conditions used for the present study are in compliance with the U.S. National Institutes of Health Guidelines for the use of experimental animals. The Animal Care and Use Committee at Oita University of Nursing and Health Sciences (Oita, Japan) also approved the method used.

Study protocol. Four groups ($n = 6$ per group) of mice (WT, TLR2^{-/-}, TLR4^{-/-} and MyD88^{-/-}) were prepared for treatments with particles. Each group was treated with sterile saline (control), PM2.5, OVA, and OVA + PM2.5. The suspension of PM2.5 particles for injection was prepared by sonicating a β -glucan (LPS) free sterile saline solution containing 0.9% NaCl (Otsuka Co., Kyoto, Japan) for 5 min with an ultrasonic disrupter, UD-201 type with micro tip (Tomy, Tokyo, Japan) under cooling conditions. Grade VII OVA (Sigma-Aldrich, St. Louis, MO) was dissolved in a sterile saline solution (Otsuka Co., Kyoto, Japan). The instillation volume of the suspension was 80 μ l/mouse for diffusing PM2.5 sample into the lungs, 0.1 mg/mouse for PM2.5 and 4 μ g per mouse for OVA. Mice treated with a polyethylene tube under 4% halothane anesthesia were intratracheally instilled with a mixed or individual solution of OVA and PM2.5 (Takeda Chemical, Osaka, Japan) 4 times at 2-week intervals. All mice (age = 14 weeks) were anesthetized by intraperitoneal injections of pentobarbital and then euthanized by exsanguination one day after the last intratracheal administration.

Bronchoalveolar lavage fluid (BALF). A previously reported method was used to count BALF and cell numbers^{15–18,22}. Briefly, after the collection of blood, tracheas were cannulated. The lungs were lavaged by syringe with two injections of sterile saline (0.8 ml) to lavage the lungs at 37 °C. Gentle aspiration was used to harvest the lavaged fluid. The mean volume retrieved was 90% of the amount instilled (1.6 ml). Fluids from the two lavages were pooled and cooled to 4 °C and then centrifuged at 1500 rpm for 10 min. The protein levels of cytokines and chemokines in the BALF were measured by using the total amount of lavages collected from each individual mouse. A hemocytometer was used to determine the total cell count of fresh fluid specimen. Assessment of differential cell counts was conducted on cytologic preparations. Slides were prepared by Cytospin (Sakura Co., Ltd., Tokyo, Japan) and then stained with Diff-Quik (International Reagents Co., Kobe, Japan). An oil immersion microscopy counted a total of 300 cells. The BALF supernatants were stored at –80 °C until analyzed for cytokines and chemokines.

Quantitative analysis of cytokines and chemokines in BALF and culture medium. An enzyme-linked immunosorbent assay (ELISA) was used to measure the cytokine protein levels in the BALF. An ELISA kit (R&D Systems Inc., Minneapolis, MN) was used to measure Interleukin (IL)-6, IL-13, eotaxin, keratinocyte chemoattractant (KC), and monocyte chemotactic protein (MCP)-1. Another ELISA kit (Endogen, Cambridge, MA) measured IL-5 and IL-12. MCP-3 was determined using an additional ELISA kit (Bender Med Systems, Burlingame, CA).

Pathological evaluation. After the BALF cells evaluation, the six mice were pathologically examined. Lungs were treated in a neutral phosphate-buffered formalin solution (10%) and then the lobes were separated (2 mm thick blocks) for paraffin embedding. Embedded blocks sectioned to a 3 μ m thickness were stained with May-Grunwald's stain solution (Nacalai tesque, Inc, Kyoto, Japan) and Giemsa's azur eosine methylene blue solution (Merck KGaA, Darmstadt, Germany) to evaluate the degree of infiltration of eosinophils or lymphocytes in the airway from proximal to distal. Sections were also stained with periodic acid-Schiff (PAS) (Waka Pure Chemicals Industry, Ltd., Osaka, Japan) for evaluation of the degree of proliferation of goblet cells in the bronchial epithelium. A Nikon ECLIPSE light microscope (Nikon Co, Tokyo, Japan) was used for pathological analysis of the inflammatory cells and epithelial cells in the airway of each lung lobe on the slides. The following scales were used to grade the degree of proliferation of goblet cells in the bronchial epithelium: 0 = not present, 1 = slight, 2 = mild, 3 = moderate, 4 = moderate to marked, and 5 = marked. These words were defined according to percentage of the airway infiltrated with goblet cells stained with PAS: "Slight" = less than 20%, "mild" = 21–40%, "moderate" = 41–60%, "moderate to marked" = 61–80%, and "marked" = more than 81%^{16–18}. One May-giemsa or PAS-stained slide per mouse was used to assess pathological changes. Two pathologists, who cross-checked the data with blinded specimens, conducted this evaluation procedure. Values are mean \pm SE ($n = 6$).

Measurement of Antigen-specific IgE and IgG1 antibodies. A Mouse OVA-IgE ELISA kit and a Mouse OVA-IgG1 ELISA kit (Shibayagi Co., Shibukawa, Japan) were used to measure OVA-specific IgE and IgG1 antibodies, respectively.

References

- Li, L. & Liu, D. J. Study on an air quality evaluation model for Beijing City under haze-fog pollution based on new ambient air quality standards. *Int. J. Environ. Res. Public Health*. **11**(9), 8909–8923 (2014).
- Lu, F. *et al.* Systematic review and meta-analysis of the adverse health effects of ambient PM2.5 and PM10 pollution in the Chinese population. *Environ. Res.* **136**, 196–204 (2015).
- Wright, J. C. *et al.* Ongoing progress in cleaning China's air: A novel outlook into pollution. *Environ. Dis.* **1**, 43–50 (2016).
- Shadie, A. M. *et al.* Ambient particulate matter induces an exacerbation of airway inflammation in experimental asthma: role of interleukin-33. *Clin. Exp. Immunol.* **177**(2), 491–499 (2014).
- Dougherty, R. H. & Fahy, J. V. Acute exacerbations of asthma: epidemiology, biology and the exacerbation-prone phenotype. *Clin. Exp. Allergy*. **39**, 193–202 (2009).
- Gavett, S. H. *et al.* Metal composition of ambient PM2.5 influences severity of allergic airways disease in mice. *Environ. Health Perspect.* **111**(12), 1471–1477 (2003).
- Mar, T. *et al.* Associations between asthma emergency visits and particulate matter sources, including diesel emissions from stationary generators in Tacoma, Washington. *Inhal. Toxicol.* **22**, 445–448 (2010).
- Zhang, S. *et al.* Short-term exposure to air pollution and morbidity of COPD and asthma in East Asian area: A systematic review and meta-analysis. *Environ. Res.* **148**, 15–23 (2016).
- Iskandar, A. *et al.* Coarse and fine particles but not ultrafine particles in urban air trigger hospital admission for asthma in children. *Thorax*. **67**, 252–257 (2012).
- Hua, J. *et al.* Acute effects of black carbon and PM2.5 on children asthma admissions: A time-series study in a Chinese city. *Sci. Total Environ.* **481**, 433–438 (2014).
- Vempilly, J. *et al.* The synergetic effect of ambient PM2.5 exposure and rhinovirus infection in airway dysfunction in asthma: a pilot observational study from the central valley of California. *Exp. Lung Res.* **39**, 434–440 (2013).

12. Delfino, R. J. *et al.* Asthma morbidity and ambient air pollution: effect modification by residential traffic-related air pollution. *Epidemiology*. **25**, 48–57 (2014).
13. Suresh, R. *et al.* Assessment of association of polycyclic aromatic hydrocarbons with bronchial asthma and oxidative stress in children: a case-control study. *Indian J. Occup. Environ. Med.* **13**, 33–37 (2009).
14. Gehring, U. *et al.* Particulate Matter Composition and Respiratory Health: The PIAMA Birth Cohort Study. *Epidemiology*. **26**(3), 300–309 (2015).
15. He, M. *et al.* Differences in allergic inflammatory responses between urban PM_{2.5} and fine particle derived from desert-dust in murine lungs. *Toxicol. Appl. Pharmacol.* **297**, 41–55 (2016).
16. He, M. *et al.* Differences in allergic inflammatory responses in murine lungs: Comparison of PM_{2.5} and coarse PM collected during the hazy events in a Chinese city. *Inhal. Toxicol.* **28**(14), 706–718 (2016).
17. He, M. *et al.* Urban particulate matter in Beijing, China, enhances allergen-induced murine lung eosinophilia. *Inhal. Toxicol.* **22**(9), 709–718 (2010).
18. He, M. *et al.* PM_{2.5}-rich dust collected from the air in Fukuoka, Kyushu, Japan, can exacerbate murine lung eosinophilia. *Inhal. Toxicol.* **27**(6), 287–299 (2015).
19. Beutler, B. Inferences, questions and possibilities in Toll-like receptor signaling. *Nature*. **430**, 257–263 (2004).
20. Schwandner, R. *et al.* Peptidoglycan and lipoteichoic acid-induced cell activation is mediated by toll-like receptor 2. *J. Biol. Chem.* **274**, 17406–17409 (1999).
21. Schnare, M. *et al.* Toll-like receptors control activation of adaptive immune responses. *Nat. Immunol.* **2**, 947–950 (2001).
22. He, M. *et al.* Desert dust induces TLR signaling to trigger Th2-dominant lung allergic inflammation via a MyD88-dependent signaling pathway. *Toxicol. Appl. Pharmacol.* **296**, 61–72 (2016).
23. Matsushima, K. Essential involvement of interleukin-8 in neutrophil recruitment in rabbits with acute experimental arthritis induced by lipopolysaccharide and interleukin-1. *Lymphokine. Cytokine. Res.* **13**, 113–116 (1994).
24. Wang, H. *et al.* The acute airway inflammation induced by PM_{2.5} exposure and the treatment of essential oils in Balb/c mice. *Sci Rep.* **7**, 44256 (2017).
25. Mariathasan, S. & Monack, D. M. Inflammasome adaptors and sensors: intracellular regulators of infection and inflammation. *Nature Reviews Immunology* **7**(1), 31–40 (2007).
26. Frantz, S. *et al.* Role of TLR-2 in the activation of nuclear factor kappaB by oxidative stress in cardiac myocytes. *J. Biol. Chem.* **276**(7), 5197–5203 (2001).
27. Ze, Y. *et al.* TiO₂ nanoparticles induced hippocampal neuroinflammation in mice. *PLoS. One.* **9**(3), e92230 (2014).
28. Tsou, T. C. *et al.* Crucial role of Toll-like receptors in the zinc/nickel-induced inflammatory response in vascular endothelial cells. *Toxicol. Appl. Pharmacol.* **273**(3), 492–499 (2013).
29. He, M. *et al.* PM_{2.5}-induced lung inflammation in mice: Differences of inflammatory response in macrophages and type II alveolar cells. *J. Appl. Toxicol.* **37**(10), 1203–1218 (2017).
30. Foster, P. S. *et al.* Interleukin 5 deficiency abolishes eosinophilia, airway hyperreactivity, and lung damage in a mouse asthma model. *J. Exp. Med.* **183**, 195–201 (1996).
31. Mosmann, T. R. & Coffman, R. L. TH1 and TH2 cells: Different patterns of lymphokine secretion lead to different functional properties. *Annu. Rev. Immunol.* **7**, 145–173 (1989).
32. Tesfaigzi, Y. Regulation of mucous cell metaplasia in bronchial asthma. *Curr. Mol. Med.* **8**, 408–415 (2008).
33. Kodama, Y. & Arashidani, K. Simplified analysis of benzo(a)pyrene in airborne particulates by High-performance liquid chromatography. *J. Chromatogr.* **261**, 103–110 (1983).

Acknowledgements

This study was supported by grants from the Global Environment Research Fund (5-1457) of the Ministry of the Environment Japan and National Nature Science Foundation of China (81302403). We appreciate the vital contribution of students at Oita University of Nursing and Health Sciences in this research.

Author Contributions

H.M. and I.T. conceived the experiments, Y.Y. and K.A. conducted the experiments, H.M. and Y.S. analysed the results. H.T. and S.G. and S.T. edited the manuscript. All authors reviewed the manuscript.

Additional Information

Competing Interests: The authors declare that they have no competing interests.

Publisher's note: Springer Nature remains neutral with regard to jurisdictional claims in published maps and institutional affiliations.



Open Access This article is licensed under a Creative Commons Attribution 4.0 International License, which permits use, sharing, adaptation, distribution and reproduction in any medium or format, as long as you give appropriate credit to the original author(s) and the source, provide a link to the Creative Commons license, and indicate if changes were made. The images or other third party material in this article are included in the article's Creative Commons license, unless indicated otherwise in a credit line to the material. If material is not included in the article's Creative Commons license and your intended use is not permitted by statutory regulation or exceeds the permitted use, you will need to obtain permission directly from the copyright holder. To view a copy of this license, visit <http://creativecommons.org/licenses/by/4.0/>.

© The Author(s) 2017